Renewable and Sustainable Energy Reviews 27 (2013) 350–361

Contents lists available at SciVerse ScienceDirect

Renewable and Sustainable Energy Reviews

journal homepage: www.elsevier.com/locate/rser

Energy and exergy analysis of the airflow inside a solar chimney

C.B. Maia [a,*], J.O. Castro Silva [a], L. Cabezas-Gómez [b], S.M. Hanriot [a], A.G. Ferreira [c]

[a] Department of Mechanical Engineering, Pontifícia Universidade Católica de Minas Gerais, Belo Horizonte, Brazil
[b] Department of Mechanical Engineering, Universidade Federal de São João Del Rey, São João Del Rey, Brazil
[c] Graduate Program of Energy Engineering, Centro Federal de Educação Tecnológica de Minas Gerais, Belo Horizonte, Brazil

ARTICLE INFO

Article history:
Received 22 April 2013
Received in revised form
6 June 2013
Accepted 16 June 2013
Available online 31 July 2013

Keywords:
Solar chimney
Exergy
Experimental analysis

ABSTRACT

Sustainable development is closely associated with the use of renewable energy resources. In order to achieve a viable development, from an environmental point of view, the energy efficiencies of processes can be increased using renewable energy resources. There is also a correlation between exergy and sustainable development, since exergy is consumed or destroyed due to irreversibilities. The solar chimney has been highlighted in studies of using solar energy to generate electric power. In this paper, the energy and exergy analyses of the airflow inside a solar chimney are presented. Using experimental data obtained in a prototype, the first and second laws of thermodynamics were used to estimate the amounts of energy and exergy lost to the surroundings and the exergetic efficiency. The dead state was defined using two different reference temperatures. The results show that the exergy losses were lower and the efficiency was higher for the lowest ambient temperature used as the dead state temperature, when compared to the instantaneous ambient temperature.

Contents

1. Introduction

Solar energy is a source of clean and renewable energy, which produces neither greenhouse gases nor hazardous waste through use. Solar energy technologies include heating, photovoltaic, thermal electricity and solar architecture. In usual thermal applications, the solar energy is applied to create steam to drive an electrical generator. A relatively new device that uses the solar energy to generate electricity is a solar chimney. The solar chimney combines the technologies of solar collectors, chimneys and turbines. The solar radiation reaches and passes through the cover, heating the soil beneath the cover, which in turn heats the air. The buoyancy forces caused by temperature gradients in the air promote upward airflow in the tower and through the centre of the lid, and this airflow can be used to drive turbines to produce electricity [1–3]. The concept was developed and a prototype was operated during the 1980s by Schaich [2]. The first practical application of a solar chimney was the development of a prototype that generated 50 kW of power built in Manzanares, Spain [4], in 1981/1982. The plant operated in the period from 1982 to 1989, and was connected to the local power

* Correspondence to: Department of Mechanical Engineering, Pontifícia Universidade Católica de Minas Gerais, PUC Minas, Av. Dom José Gaspar, 500, Prédio 10, Coração Eucarístico, CEP 30535-910, Belo Horizonte, MG, Brazil.
Tel.: +55 31 33194323; fax: +55 31 33194910.
E-mail addresses: cristiana@pucminas.br, cbmaia@oi.com.br (C.B. Maia).

1364-0321/$ - see front matter © 2013 Elsevier Ltd. All rights reserved.
http://dx.doi.org/10.1016/j.rser.2013.06.020

supply between 1986 and 1989 [3]. The operation and results of operational tests of the prototype are described by Haaf et al. [5] and Haaf [6]. No complete solar power plant using a solar chimney has been built so far, but a project of 200 MW is being developed in Australia [7].

Economic evaluations based on measurements taken and the operational experience gained during the Manzanares project showed that 100 MW plants are economically competitive to conventional power plants [8]. To evaluate the viability of new projects, cost models for large-scale solar chimney power plants were developed. Schlaich [3] presented energy production costs and compared these values to coal and combined cycle power plants based on equal and common methods. Schlaich et al. [9] presented cost values for the solar chimney components and levelised electricity costs for various plants for fixed economic parameters. Bernardes [10] determined the costs for plants of several sizes and investigated the sensitivity of the levelised electricity costs to economic parameters. Fluri et al. [11] presented a more detailed cost model, including a model for the power conversion unit and compared the results to the literature models.

Many works have been developed on the study of solar chimneys. Zhou et al. [12] presented a comprehensive state of the art review of research and development of solar chimneys for power generation. The authors reviewed experimental and theoretical studies, concerning both the physical and economic aspects of developments, and concluded that solar chimney power technology will possibly play an important role in world development in the future.

Most theoretical works about solar chimneys found in literature deal only with the analysis based on the first law of thermodynamics. In recent years, growing attention has been given to analysis of drying processes using the second law of thermodynamics [13-19]. However, the only research developed with a second law of thermodynamics analysis for a SCPP was performed by Petela [20]. The author presented a thermodynamic analysis of energy distribution in the whole system using an exergetic approach. The objective was to outline a simplified interpretative mathematical model of the solar chimney. However, the results presented were based on a series of assumptions, not on experimental data. The main objective of the present paper is to analyse the thermodynamic behaviour of a solar chimney prototype without any products inside. Applying the first and second laws of thermodynamics, the energy transferred to the airflow and the exergy lost to the surroundings, as well as the exergetic efficiency, and the energy and exergy rates inside the chimney are estimated. The results obtained and presented herein are from experimental data from a 4-day test in which the solar radiation, ambient, ground and outlet airflow temperatures, inlet and outlet humidities and the outlet mass flow rate were measured. It is important to mention that the prototype has small dimensions in comparison to the dimensions of solar chimney power plants, since the main purpose of the prototype was the drying of agricultural products.

2. Literature review

There is now a wide and growing body of literature on the study of solar chimneys. The outstanding works are discussed in this section.

2.1. Mathematical models

Several studies about solar chimneys have been performed to predict the behaviour of the airflow inside a solar chimney, using both computational fluid dynamics (CFD) simulations and global analysis.

Bernardes et al. [21] presented a theoretical analysis of the laminar natural convection inside the device, for steady state conditions. After this study, Maia et al. [22] improved this model to take into account unsteady turbulent conditions, validating the results through comparison with experimental data. Chergui et al. [23] developed a finite volume method to discretise the Navier–Stokes and energy equations for a laminar natural convection airflow. A mesh size of 1/22 (24×24 cells) was used and the results were validated with respect to the Vahl Davis benchmark solution [24]. Pastohr et al. [25] modelled the problem using the software Fluent. The Reynolds-averaged Navier–Stokes equations were numerically solved for the airflow, with a simple turbine model and the heat conduction equation to predict the ground surface temperature. Ming et al. [26] solved the Navier–Stokes and energy equations for the airflow, as well as transport equations for the turbulent variables. Different mathematical models for the collector, the chimney, and the energy storage layer under the solar chimney were developed to be used as boundary conditions for the aforementioned equations. The Manzanares prototype was selected as a physical model for the numerical simulation. Tingzhen et al. [27] carried out numerical simulations on solar chimney systems using the CFD techniques. The influence of solar radiation and pressure drop across the turbine on the flow and heat transfer, output power, and energy loss of the solar chimney power plant system (SCPP) were analysed. The numerical simulation results revealed that, for a solar chimney with a chimney 400 m in height and with a collector 1500 m in radius and a 5-blade turbine, the maximum power output and turbine efficiency is about 10 MW and 50%, respectively.

Koonsrisuk and Chitsomboon [28] showed that dynamic similarity for scaled models and a full-scale solar chimney prototype is achievable, while maintaining the same insolation. Nevertheless, only a partial geometrical similarity is allowed. Experiments were not performed to confirm the validity of the study. Instead, data similarities between the model and a prototype were compared using numerical results provided by CFD analysis. Later, the same authors [29] used dimensional analysis to combine eight primitive variables into one dimensionless parameter to establish dynamic similarity between a prototype and its scaled models. This dimensionless parameter was interpreted as the total kinetic energy scaled by the buoyant energy of the rising hot air. To validate the proposed dimensionless parameter, three classes of scaled models were set up and the governing equations were solved using CFD analysis. Xu et al. [1] developed a two dimensional model for the solar chimney and an energy storage layer under the device, evaluating the influences of solar radiation, turbine pressure drop and efficiency on the flow and heat transfer, output power, and energy loss of the system. The Fluent software was used to solve the governing equations and the model was validated with experimental results from the Manzanares prototype. Sangi et al. [30] described a detailed numerical analysis of a SCPP, using Fluent software to simulate a two-dimensional axisymmetric model, with the standard k-epsilon turbulence model. The model was validated with data from the Manzanares prototype. The authors also developed an expression for the static pressure inside the collector.

The airflow generated in a solar chimney is commonly used to drive a wind turbine and to generate electricity. Therefore, the electrical output is the most important characteristic in a SCPP. The prediction of its performance and the influence of the physical dimensions on a solar chimney's performance have been studied by several researchers. Asnaghi and Ladjevardi [31] stated that the most important physical elements in a solar chimney are the tower dimensions as they cause the most significant influence on

the flow patterns. Another important factor is the collector's roof shape. Also, research has shown that greater power production is feasible by optimising the collector's roof shape and height. Bernardes et al. [32] developed a model to estimate the power output of solar chimneys and examine the effects of various ambient conditions and structural dimensions on the power output. The model was validated using results from the Manzanares pilot plant. Koonsrisuk and Chitsomboon [33] compared the predictions of performances of SCPP by using five simple theoretical models proposed in the literature. The authors performed CFD simulations and compared the results with theoretical predictions. Analytical approaches are also found in literature for estimation of the airflow parameters of SCPP. Pretorius and Kröger [34] evaluated the influence of several convective heat transfer coefficients, turbine inlet loss coefficients, collector roof glasses and various types of soil on the performance of a SCPP. Fluri and Von Backström [35] determined the SCPP power production spectrum over a year and determined the required characteristics of the turbine(s) to match the plant and compared three power conversion unit configurations. Nizetic and Klarin [36] presented a mathematical model based on a simplified thermodynamic analysis of the overall solar chimney cycle to estimate the optimal factor of turbine pressure drop. The authors theorised that even for constant solar irradiation, the pressure potential is not fixed, but a function of the air temperature increase in the collector. Li et al. [37] described a comprehensive theoretical model for the performance evaluation of a solar chimney power plant, verified by the experimental data from the Spanish prototype. The authors stated that there is a maximum power output under a given solar radiation condition and that there is a limitation on the maximum collector radius for the maximum attainable power of the SCPP; whereas no such limitation exists for chimney height in terms of contemporary construction technology. Hamdan [38] provided a mathematical thermal model to evaluate the performance of a SCPP, based on its dimensions and operating conditions. The model was developed using a modified Bernoulli equation with buoyancy effect and an ideal gas equation. Koonsrisuk and Chitsomboon [39] developed a theoretical model to evaluate the performance of SCPP. The relationships between the pressure ratio and the mass flow rate and between the temperature rise across the collector and the power output were also presented.

2.2. Worldwide studies

Many attempts have been made to evaluate solar chimneys in some parts of the world. To the best knowledge of the authors, there was only one prototype built in South America. Maia et al. [40] described an experimental study of a prototype built in Brazil with a solar collector with a 25 m diameter and a 13 m high tower. Since the estimated power was very low, a turbine was not installed. Instead, the hot airflow generated was used to dry agricultural products. Ferreira et al. [41] investigated the technical feasibility of the device as a dryer. Drying tests of coffee grains, bananas and tomatoes were performed inside the dryer.

Kasaeian et al. [42] conducted an experimental investigation of climatic effects on the efficiency of a SCPP. The solar chimney in pilot scale was built in Iran, with a chimney height of 12 m and a collector with a 10 m diameter. Sangi [43] estimated the potential for electrical energy production by a solar chimney in selected regions of Iran. A simplified mathematical model based on the energy balance was developed to estimate the power output of solar chimneys, as well as to examine the effect of various ambient conditions and structural dimensions on power generation. Asnaghi and Ladjevardi [31] performed numerical simulations to investigate SCPP in 12 selected locations in Iran, comparing power generation for each region. An analysis of overall performance of a device with similar fundamental dimensions to the Manzanares prototype was provided, considering the radiation variations through the year in the selected regions. Gholamalizadeh and Mansouri [44] presented a comprehensive analysis to predict the performance of a SCPP in Kerman, Iran. Analytical and numerical models were developed, and the results were compared to experimental data from the Manzanares prototype.

Dai et al. [2] evaluated a SCPP to be constructed in northwestern China to provide electric power for remote villages. The performance of the device was compared for three possible locations. Results showed that a prototype 200 m high and with a 500 m collector diameter was expected to produce 110–190 kW electric power. Zhou et al. [45] developed a small-scale prototype of solar chimney thermal power plant in China, 8 m high and with a radius that may vary from 1 m to 5 m. A simulation study was carried out to investigate the performance of the system based on a mathematical model. With the reduced dimensions, the device was able to generate up to approximately 5.5 W. Zhou et al. [46] built a prototype in China, consisting of an air collector 10 m in diameter and an 8 m tall chimney. The temperature distribution was presented for a typical cool day and for a typical warm day. The results showed a temperature difference between the collector outlet and the ambient up to 24.1 °C. Zhou et al. [47] developed a mathematical model for the evaluation of the performance of a solar chimney to generate electric power to run the railway lines in the Qinghai–Tibet Plateau and to supply the developed regions by high-voltage lines. The results indicated that when 10–20% of land in the plateau is used for solar chimney power plants, the yearly power could account for 10.7–21.3% of China's energy consumption in 2008.

Onyango and Ochieng [48] evaluated the potential of solar chimneys for application in developing countries, highlighting its appropriateness to rural villages. Nizeticet al [49] evaluated the viability of implementing SCPP in the Mediterranean region through a cost analysis. A device 550 m high with a collector with a 1250 m diameter would generate 2.8–6.2 MW of power. Larbi et al. [50] presented a performance analysis of a prototype expected to produce between 140 kW and 200 kW of electricity in Algeria's south-western region. Hamdan [7] developed a simplified thermodynamic analytical model to analyse the feasibility of solar chimney power plants for the Arabian Gulf region. Ketlogetswe et al. [51] described an experimental study of a solar chimney with a collection area of approximately 160 m^2 built in Botswana (Southern Africa). The tower had an inner diameter of 2 m and a height of 22 m. The main parameters evaluated were the air velocity, temperature and solar radiation. The results were obtained under different operational conditions: with a turbine installed, without the turbine and without the turbine and the diffuser. The range of temperature difference varied from about 2.1 to 7.5 °C. Air velocity was in the range of 1–2.5 m/s with the diffuser installed and 2–4 m/s with the diffuser removed. Other small-scale prototypes were developed. Kirsst [52] built a 10 W prototype in America. Kulunk [53] built a 2 m high prototype in Turkey, able to generate 0.14 W.

3. Experimental setup

A prototype of a solar chimney was built in Belo Horizonte (Brazil). The tower was 12.3 m high, and the collector diameter was 25 m. The height of the collector varied from 0.05 m in the entrance to 0.5 m in the symmetry axis (Fig. 1).

The temperature, velocity and humidity ratio of the air, and the ambient temperature and solar radiation were measured over a 4-day period. Despite several papers (e.g.,[42,46]) presenting results for a 1-day period or instantaneous data, it was chosen to show

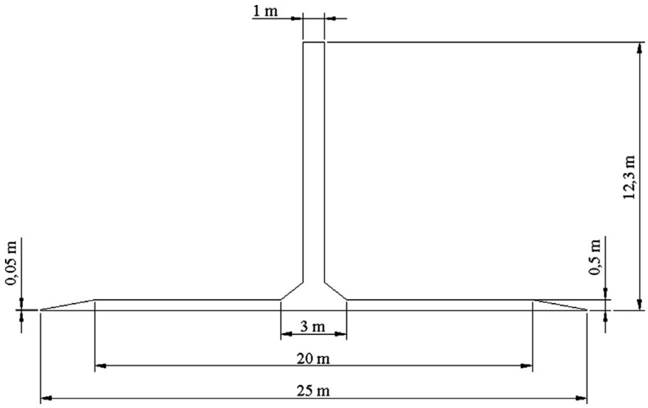


Fig. 1. Schematics of the prototype.

the results for a 4-day period in order to highlight the influence of the climatic parameters on the airflow. The period chosen shows opposite behaviours concerning the incident solar radiation and clearness indexes. The ambient, ground and outlet airflow temperatures were measured with *K* thermocouples (uncertainty of 1 °C). Eppley Black and White Pyranometers Model 8–48 were used to determine solar radiation (global uncertainty of 5%). Propeller Homis anemometers were used to measure the velocity in the tower. The global uncertainty was 6%. Capacitive psychrometers were used to measure the ambient relative humidity and the relative humidity of the airflow (uncertainty of 6%). The analogue voltage or current signals from the humidity, temperature, velocity and solar radiation measurement sensors were converted into digital signals through ADAMS 4018 Modules in a data acquisition system.

The ambient temperature and relative humidity were measured outside the device. Thermocouples and psychrometers were also positioned in the inlet and outlet of the device. Anemometers were used to measure the velocity along a cross section of the tower. A numerical integration was performed to determine the mass flow rate of the airflow. The global and diffuse components of solar radiation were measured in a horizontal plane outside the prototype.

The experiments were conducted in late autumn in Brazil, with maximum and minimum air temperatures around 27.3 °C and 8.4 °C, respectively. The air's relative humidity varied between 25.6% and 90.6% and the maximum solar radiation was 1065 W/m^2.

4. Modelling

The balance equations set were developed according to models from the literature [15,54]. The balance equations were applied to find the work and heat interactions, the exergy rates, the exergy losses, and the exergy efficiency.

The general equation of mass conservation can be expressed in the rate form as

$$\dot{m}_{ai} = \dot{m}_{ao} \quad (1)$$

where $\dot{m}_{ai}$ and $\dot{m}_{ao}$ represent the inlet and outlet mass flows of the airflow, respectively.

For the drying air and moisture, the mass conservation is expressed as

$$\dot{m}_{wi} + \dot{m}_{mp} = \dot{m}_{wo} \quad (2)$$

$\dot{m}_{wi}$ and $\dot{m}_{wo}$ represent the inlet and outlet mass flows of humidity, respectively. $\dot{m}_{mp}$ is the mass flow of the moisture from the ground. The mass conservation for the moisture can also be rewritten in terms of the inflow and outflow specific humidities, respectively, ω_{ai} and ω_{ao}, as

$$\dot{m}_{ai}\omega_{ai} + \dot{m}_{mp} = \dot{m}_{ao}\omega_{ao} \quad (3)$$

The general energy balance can be expressed as the total energy inputs equal to total energy outputs:

$$\sum \dot{E}_{in} = \sum \dot{E}_{out} \quad (4)$$

or

$$\dot{Q} = \dot{m}_{ao}\left(h_{ao} + \frac{V_{ao}^2}{2}\right) - \dot{m}_{ai}\left(h_{ai} + \frac{V_{ai}^2}{2}\right) \quad (5)$$

The previous equation is used to determine the net heat rate $\dot{Q}$. The energy utilisation rate is neglected, since there is no turbine in the system. V_{ai} and V_{ao} represent the air velocity in the inlet and outlet of the system, respectively. The specific enthalpies of the air in the inlet and outlet, h_{ai} and h_{ao}, were determined using the correlations available in the EES (Engineering Equation Solver) software:

The general exergy balance can be written as follows:

$$\sum \dot{E}x_{in} - \sum \dot{E}x_{out} = \sum \dot{E}x_{lost} \quad (6)$$

In the previous equation, $\dot{E}x_{in}$, $\dot{E}x_{out}$ and $\dot{E}x_{lost}$ represent the exergy inflow, outflow, and the exergy loss respectively. This equation can be also expressed as

$$\dot{E}x_{heat} - \dot{E}x_{work} + \dot{E}x_{mass,in} - \dot{E}x_{mass,out} = \dot{E}x_{lost} \quad (7)$$

With the exergy flow rate due to the heat transfer given as

$$\dot{E}x_{heat} = \left(1 - \frac{T_0}{T_k}\right)\dot{Q} \quad (8)$$

$\dot{Q}$ is the heat transfer rate through the boundary at temperature T_k at location k, considered as the ground temperature. T_0 represents the dead state temperature. For the system considered, the exergy rate due to work interactions $\dot{E}x_{work}$ can be neglected.

The exergy inflow $\dot{E}x_{mass,in}$ is only due to the airflow entering the system, and the exergy outflow $\dot{E}x_{mass,out}$ is due to the airflow leaving the system and to the water removed from the ground, $\dot{E}x_w$.

$$\dot{E}x_{mass,in} = \dot{m}_{ai}\psi_{ai} \quad (9)$$

$$\dot{E}x_{mass,out} = \dot{m}_{ao}\psi_{ao} + \dot{E}x_w \quad (10)$$

where

$$\dot{E}x_w = \dot{m}_{mp}\psi_{wo} \quad (11)$$

Therefore, the exergy outflow is

$$\dot{E}x_{mass,out} = \dot{m}_{ao}\psi_{ao} + \dot{m}_{mp}\psi_{wo} \quad (12)$$

The specific flow exergy Ψ is calculated in a generic form as

$$\psi = (h - h_0) - T_0(s - s_0) \quad (13)$$

where h is the specific enthalpy and s is the specific entropy.

The inlet and outlet specific flow exergies are calculated by [55]

$$\psi_{ai} = (C_{p,ai} + \omega_{ai}C_{p,v})T_0\left(\frac{T_{ai}}{T_0} - 1 - \ln\frac{T_{ai}}{T_0}\right) + (1 + 1.6078\omega_{ai})R_aT_0\ln\frac{P_{ai}}{P_0}$$
$$+ R_aT_0\left[(1 + 1.6078\omega_{ai})\ln\left(\frac{1 + 1.6078\omega_0}{1 + 1.6078\omega_{ai}}\right) + 1.6078\omega_{ai}\ln\frac{\omega_{ai}}{\omega_0}\right] \quad (14)$$

$$\psi_{ao} = (C_{p,ao} + \omega_{ao}C_{p,v})T_0\left(\frac{T_{ao}}{T_0} - 1 - \ln\frac{T_{ao}}{T_0}\right)$$
$$+ (1 + 1.6078\omega_{ao})R_aT_0\ln\frac{P_{ao}}{P_0}$$

$$+R_a T_0\left[(1+1.6078\omega_{ao})\ln\left(\frac{1+1.6078\omega_0}{1+1.6078\omega_{ao}}\right)+1.6078\omega_{ao}\ln\frac{\omega_{ao}}{\omega_0}\right] \quad (15)$$

where R_a is the ideal air constant, P_o is the dead state pressure, P_{ai} and P_{ao} are the air pressure in the inlet and outlet, respectively, and T_{ai} and T_{ao} are the air temperatures in the inlet and outlet, respectively. $C_{p,v}$ is the specific heat of the water vapour, and ω_0 is the specific humidity of the flow in dead state.

The outlet specific flow exergy of the water, considered as an incompressible substance, is given by

$$\psi_{wo}=C\left(T_{ao}-T_0-T_0\ln\frac{T_{ao}}{T_0}\right) \quad (16)$$

It is assumed that the air and water leave the system at the same temperature, T_{ao}. In the previous equation, C is the specific heat of water.

Therefore, the exergy loss is determined by

$$\dot{E}x_{lost}=\left(1-\frac{T_0}{T_k}\right)\dot{Q}+\dot{m}_{ai}\psi_{ai}-\dot{m}_{ao}\psi_{ao}-\dot{m}_{mp}\psi_{wo} \quad (17)$$

The irreversibility rate I is given by

$$I=\dot{E}x_{lost} \quad (18)$$

The exergy efficiency ε is defined as the ratio of total exergy output to total exergy input:

$$\varepsilon=\frac{\dot{E}x_{out}}{\dot{E}x_{in}}=1-\frac{\dot{E}x_{lost}}{\dot{E}x_{in}} \quad (19)$$

Van Gool [56] proposed that maximum improvement in the exergy efficiency for a process or system is achieved when the exergy loss or irreversibility is minimised. Therefore, it is useful to use the concept of exergetic improvement potential, defined as

$$I\dot{P}=(1-\varepsilon)(\dot{E}x_{in}-\dot{E}x_{out}) \quad (20)$$

Exergy is always evaluated with respect to a reference environment, the dead state. When a system is in thermodynamic equilibrium with the environment, the state of the system is called the dead state due to the fact that the exergy is zero. According to [54], dead state is an arbitrary reference state. Usually, results are presented in literature for steady state conditions. In this paper, unsteady state conditions were evaluated. The reference temperature (selected as the dead state temperature) was the inlet temperature. Since the inlet temperature varied during the tests, two dead states were defined and the results were compared. Both dead states were selected as a system with zero velocity and elevation relative to coordinates in the environment, with the local ambient atmospheric pressure (91.5 kPa). The main difference between the definitions was the temperature: in the first, the selected temperature was the minimum ambient temperature (approximately 8.5 °C) during the experimental tests performed; in the second dead state, the temperature was the instantaneous ambient temperature. It can be noticed that in all the above balance equations (Eqs. (2)–(6)) the cumulative terms are neglected, considering that even if the thermodynamics properties change with time, its temporal derivatives are null.

5. Results and discussion

Fig. 2 presents the total and diffuse components of solar radiation measured during the four days of tests. The average clearness index (the ratio of the daily radiation to the extra-terrestrial radiation of the day [57]) was determined for each day, obtaining values of 0.68, 0.63, 0.72 and 0.53, respectively, for the first, second, third and fourth day of tests. It can be seen that higher clearness indexes correspond to clearer days.

Fig. 3 shows the inlet and outlet temperatures of the airflow and the ground temperature. As expected, the temperature and

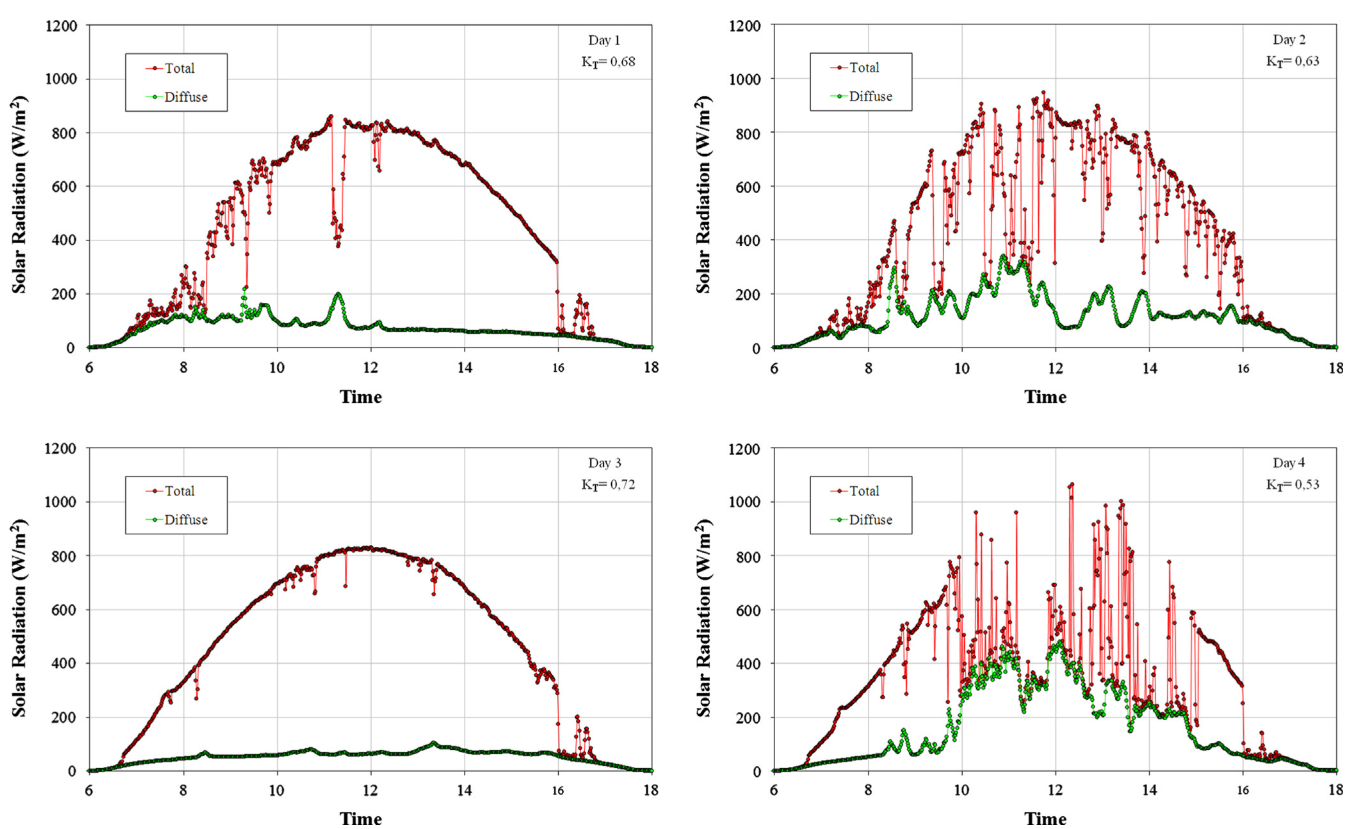


Fig. 2. Total and diffuse components of solar radiation.

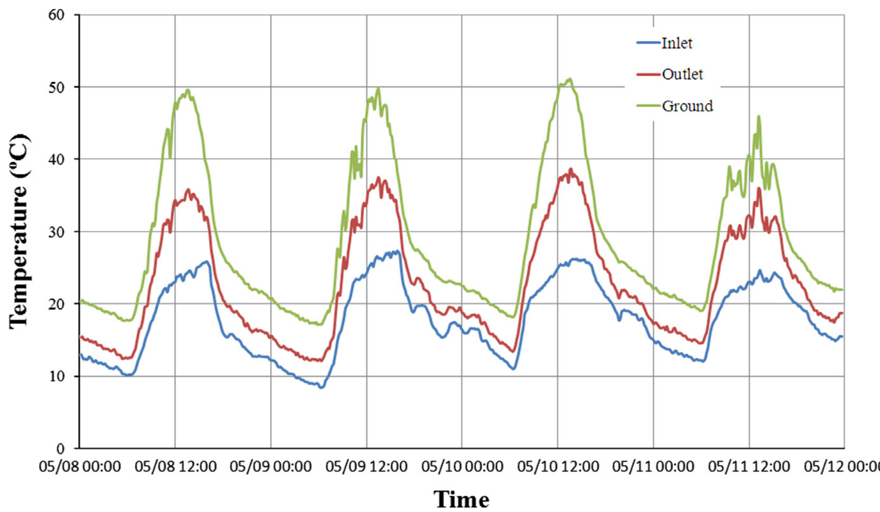


Fig. 3. Temperature distribution.

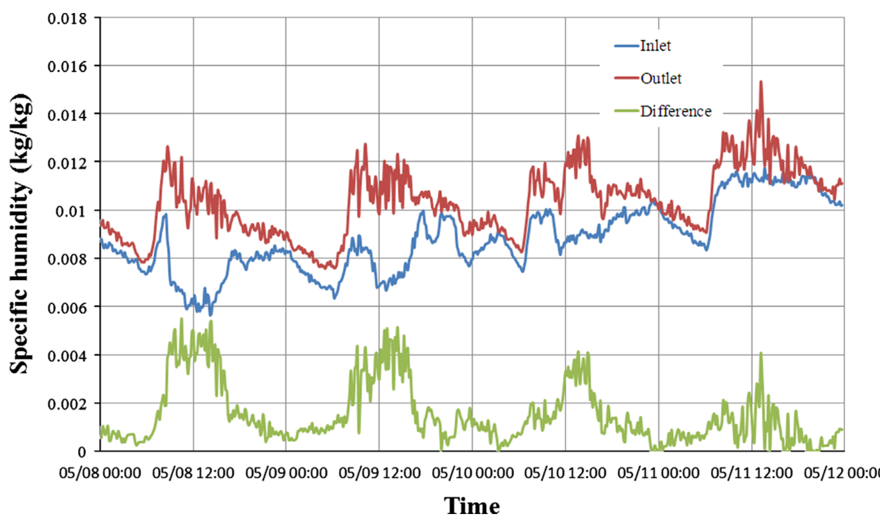


Fig. 4. Specific humidity distribution.

total solar radiation profiles exhibit a similar behaviour. Higher temperatures are observed for higher clearness indexes. It can also be seen that the solar chimney is able to operate at night. During the day, when there is incidence of solar radiation, ground surface temperature is higher than the temperature of the deeper layers. Therefore, heat is conducted from the surface to the deeper layers of the ground and stored there as heat. At night, the temperature of the ground surface decreases, becoming lower than the deeper layers' temperatures. Thus, heat flux goes in the opposite direction [40].

Fig. 4 shows the inlet and outlet airflow specific humidities. It can be seen that the outlet humidity is greater than the inlet humidity. Since the prototype ground was not sealed, the difference can be explained by the removal of water from the ground by the airflow. A difference between the inlet and outlet airflow specific humidities is also observed. During the day, the ambient temperatures were higher, causing a decrease in the specific humidity in the inlet. Since the air entered the device with a lower specific humidity, it was easier to remove water from the ground, increasing the difference in the specific humidities in the inlet and outlet. At night, the opposite behaviour was found.

The airflow is produced by buoyancy forces resulting from a greenhouse effect inside the collector. Therefore, the velocity depends on the difference between the ground and the airflow temperature, which depends on the incident solar radiation. Fig. 5 presents the mass flow rate during the whole test. The higher values were obtained when the solar radiation and the temperature were higher, but there is also an airflow at night, due to the temperature difference observed in Fig. 3. The average velocity in the tower varied from 1.1 m/s to 2.7 m/s, corresponding to Reynolds numbers (in the tower) from 6.4×10^4 to 1.5×10^5, showing characteristics of turbulent airflows.

Fig. 6 shows the heat transfer rate from the ground to the airflow. As expected, the heat transfer rate exhibits a similar behaviour to the other parameters, with higher values associated to higher solar radiation values. There is also a small portion of heat being transferred at night, when there is no incidence of solar radiation.

As previously discussed, the dead state is an arbitrary state of reference. In this work, two dead states were selected. Fig. 7 presents the exergy rates for a fixed value of the temperature of the dead state. The temperature was selected as the minimum value of the ambient temperature obtained during the tests. Fig. 8 presents the exergy rates for the dead state temperature defined as the ambient temperature, which varied from 8.4 °C to 27.3 °C.

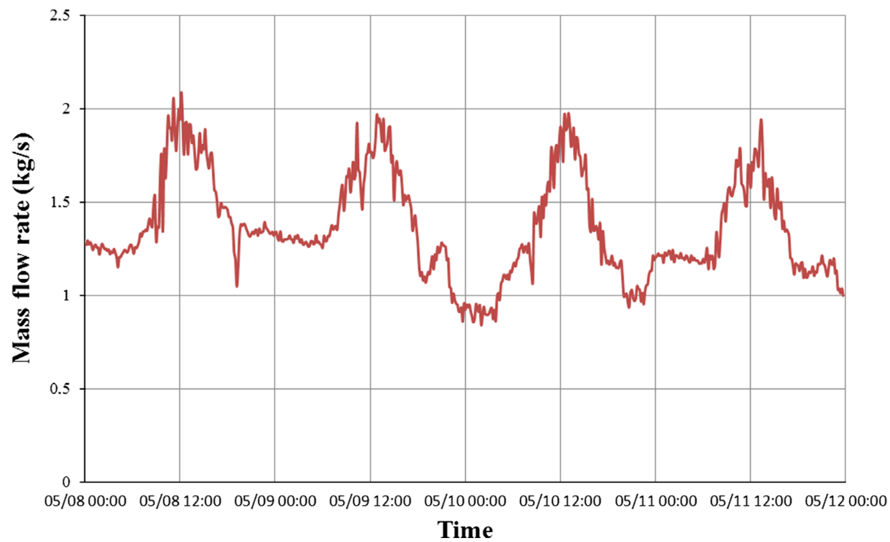


Fig. 5. Mass flow rate distribution.

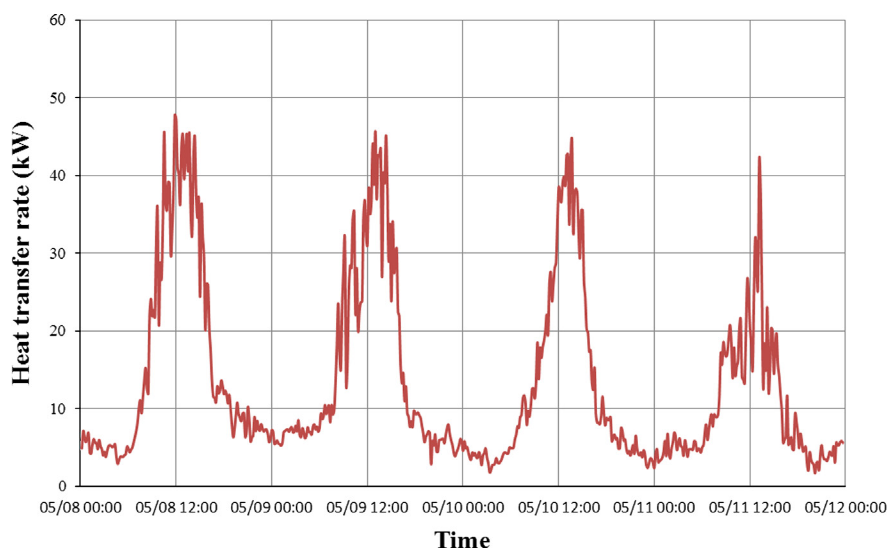


Fig. 6. Heat transfer rate distribution.

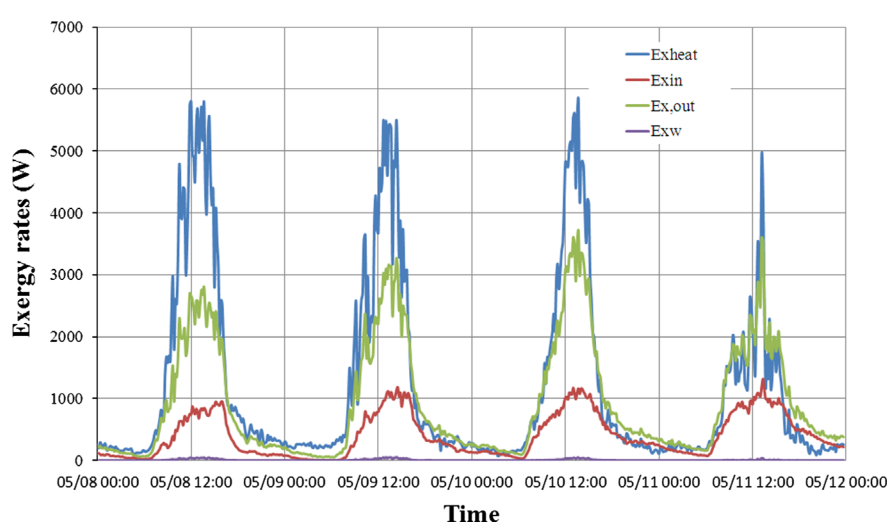


Fig. 7. Exergy as a function of time for the dead state selected with a fixed temperature.

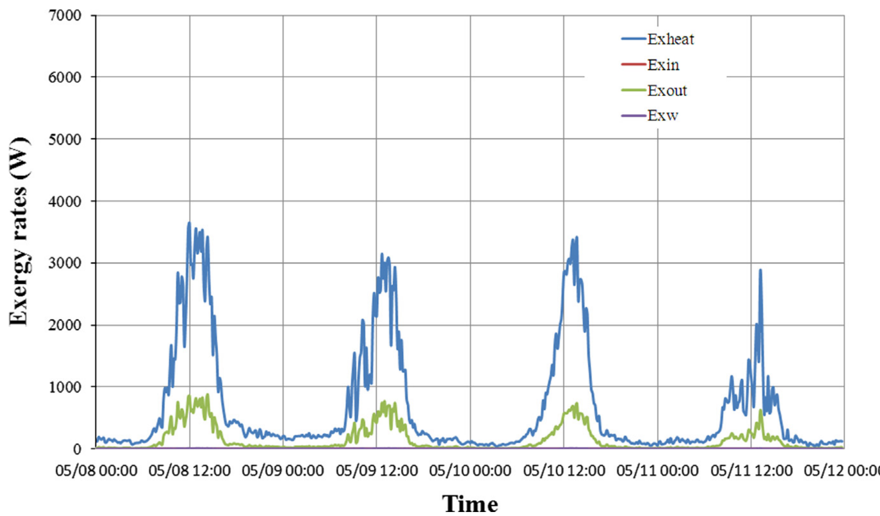


Fig. 8. Exergy as a function of time for the dead state selected with ambient temperature.

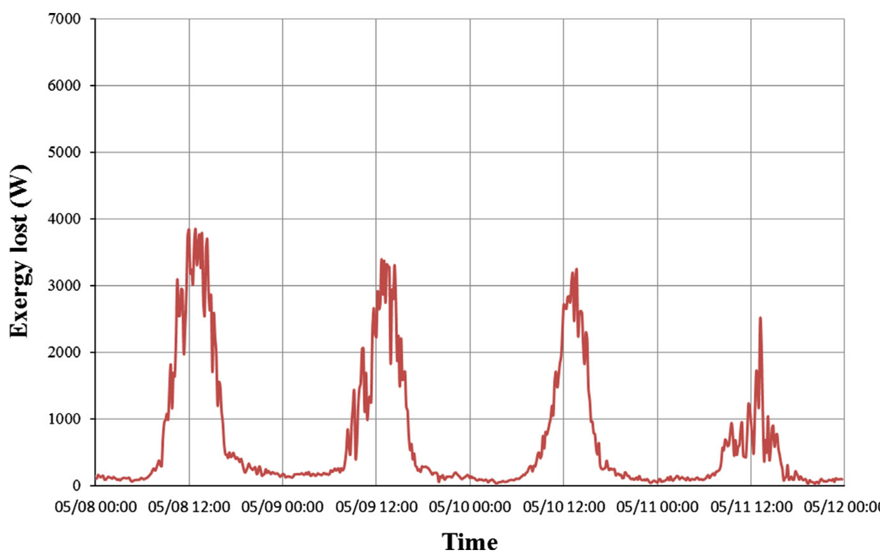


Fig. 9. Exergy losses as a function of time for the dead state selected with a fixed temperature.

The general behaviour of the exergy rates is similar to the behaviour of the temperature. The exergy rates are higher for a constant temperature of the dead state, since a higher amount of work could be produced as the system comes to equilibrium with the reference environment at a lower temperature. In Figs. 7 and 8, the higher exergy rates were found for the exergy flow rates due to heat transfer, and the lower exergy rates were found for the exergy rates of the water removed from the ground. Therefore, the higher exergy rates are associated to higher solar radiation levels. When the ambient temperature was selected as the dead state temperature, the exergy rate of the inlet mass flow is always zero, since the reference state is the inlet air.

Figs. 9 and 10 present the exergy losses for a fixed value of the temperature of the dead state and for the dead state temperature defined as the ambient temperature, respectively. The losses are very significant, and the higher losses correspond to higher solar radiation levels, due to the higher heat transfer rates achieved. Since the hot airflow generated was only used to remove humidity from the ground, not being used to drive any engine or to dry agricultural products, the heat was not used, increasing the exergetic losses. It is also seen that the losses are more pronounced for a fixed dead state temperature due to the lower comparison level as it is more difficult to enter into equilibrium with a lower reference environment and/or because the exergy rates (mainly related to the exergy rates due to heat transfer) are higher in this case.

Figs. 11 and 12 present the exergetic efficiency for a fixed value of the temperature of the dead state and for the dead state temperature defined as the ambient temperature, respectively. It can be seen that the efficiencies are higher for a fixed value of the dead state temperature, since the reference temperature is lower than the ambient temperature for the majority of the time. When analysing the temporal change in temperatures, it can be seen that the exergetic efficiency is continuously varying, with higher values obtained for the last day of tests. In the last day, lower solar radiation levels were found, as well as lower heat transfer rates. Nevertheless, the exergetic losses were lower, increasing the exergetic efficiency.

No data in the literature was found for a similar configuration of the prototype used in these experiments. Hamdan [7] presented a simplified thermodynamics analytical model for steady airflow inside a solar chimney power plant. In order to validate the

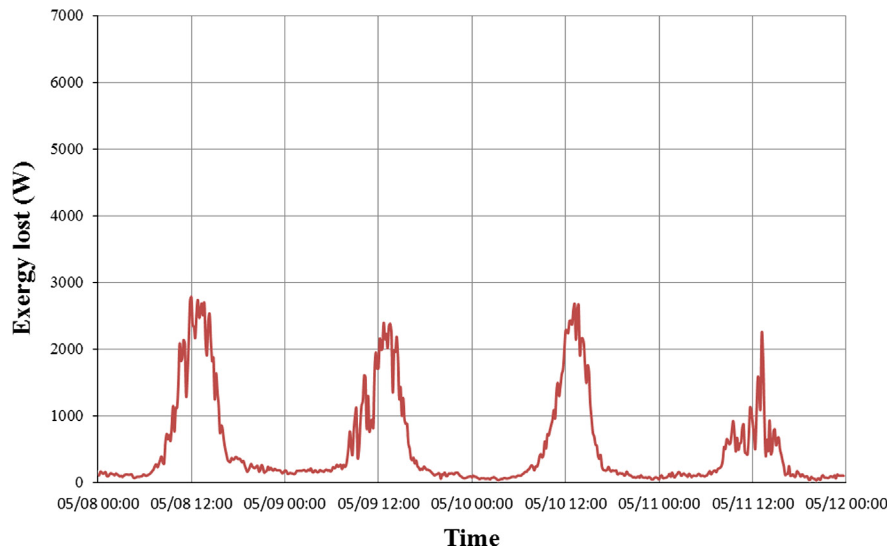


Fig. 10. Exergy losses as a function of time for the dead state selected with ambient temperature.

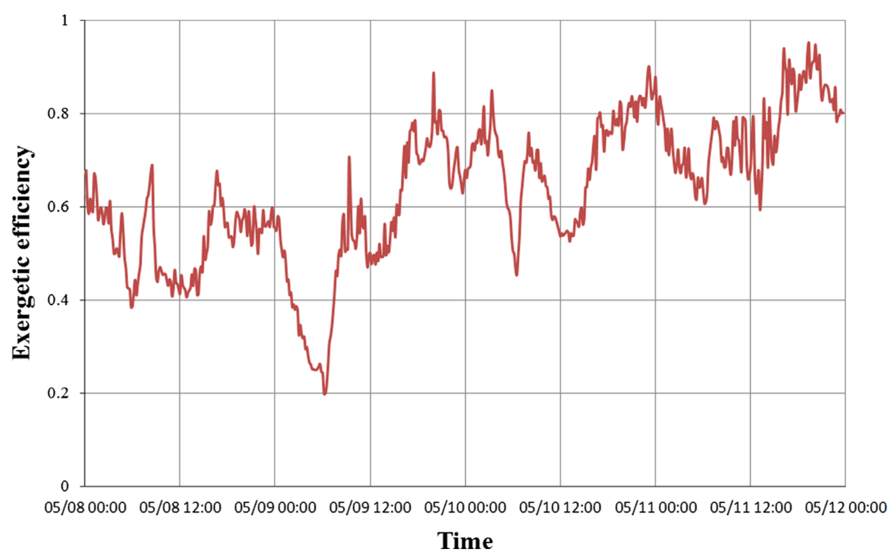


Fig. 11. Exergetic efficiency as a function of time for the dead state selected with a fixed temperature.

developed model, the results were compared against published experimental data, with good agreement for the power generated as a function of geometric and operational parameters. The second-law efficiency of the system was determined, based on the developed model, with values between 15% and 38%, depending on the chimney height (between 500 m and 1000 m). It was observed that the second-law efficiency increases with the chimney height. The efficiency defined is related to the expected turbine power, as also suggested by Saidur et al. [58] for solar power plants. Nevertheless, the results obtained by Hamdan [7] cannot be compared with the efficiencies obtained in this paper, since, in this paper, the solar chimney does not have a turbine and the dimensions of the prototypes were not alike.

Figs. 13 and 14 present the improvement potential for a fixed value of the temperature of the dead state and for the dead state temperature defined as the ambient temperature, respectively. As expected, the improvement potential is lower for a fixed temperature of the dead state, since the efficiencies are higher for this condition. The relatively higher values of the improvement potential can be explained by the fact that the airflow is only being used to remove water from the ground. Therefore, there is a great potential of exergy to be harnessed, reducing the exergy losses.

As a core outcome of the results, it can be said that higher solar radiation leads to higher temperatures and mass flow rates, resulting in higher the heat transfer rates. Since the higher exergy rates are due to the heat transfer rates, the higher exergy losses and the lower exergetic efficiencies can be related to the higher solar radiation levels. However, it must be clear that these results are valid for this prototype, where the heat transfer rate was only used to remove water from the ground.

The temperature defined for the dead state played an important role on the exergetic analysis. When a fixed temperature was selected, instead of the ambient temperature (which varied during the tests), higher exergy rates and exergetic efficiencies were found. The exergetic losses were significant due to the fact that the hot airflow was only used to remove water from the ground; nevertheless, the main goal of this paper was to analyse the

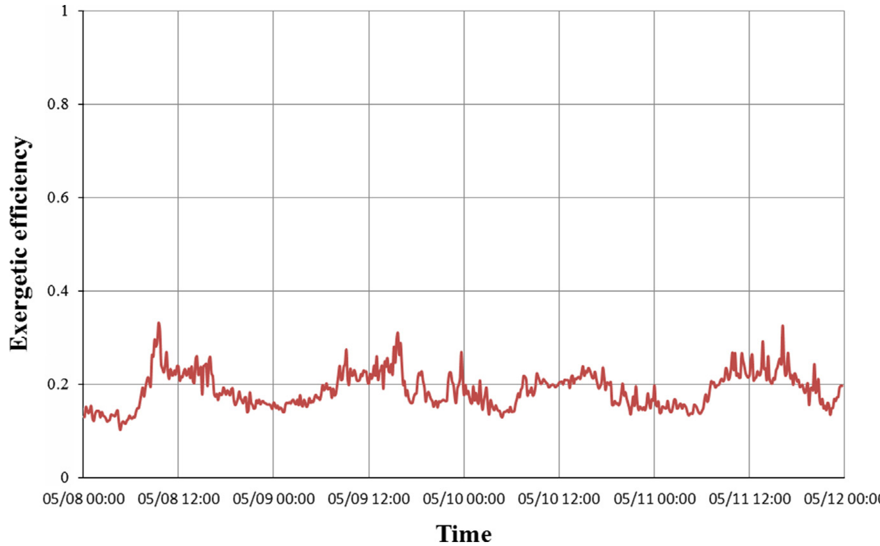


Fig. 12. Exergetic efficiency as a function of time for the dead state selected with ambient temperature.

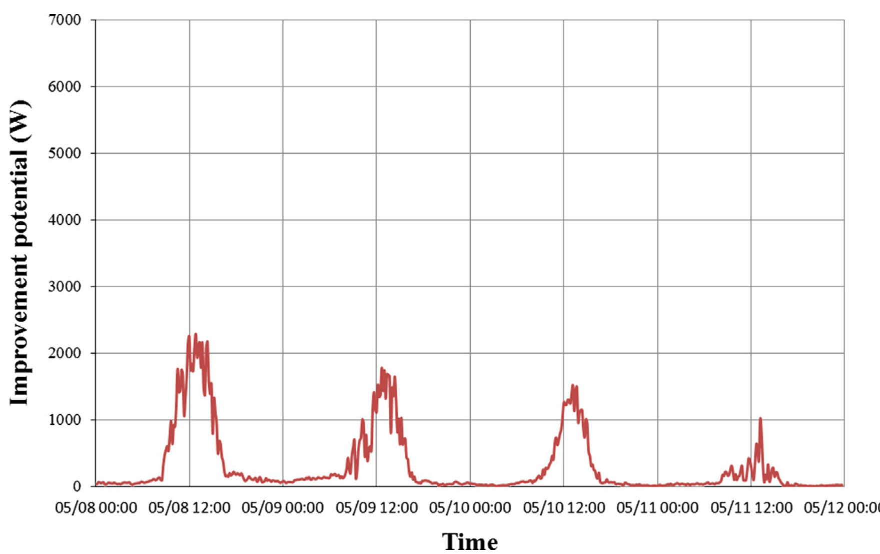


Fig. 13. Improvement potential as a function of time for the dead state selected with a fixed temperature.

behaviour of the airflow inside the solar chimney with no products inside. It is important to note that, in spite of this, the hot airflow generated in a solar chimney can be used to drive a turbine in solar chimney power plants or to dry agricultural products in a smaller prototype. In a solar chimney power plant, it is shown that higher solar radiation levels increase the power output and the energetic efficiency of the system [12,28]. In a drying process, the most important parameter of the drying efficiency is the difference between the relative humidities of the airflow and the products to be dried. An increase of the source of energy (in this case, the solar energy) increases the airflow temperature, which decreases the relative humidity of the air, improving the drying characteristics [59].

6. Conclusions

In order to perform an exergetic and energetic analysis of the airflow in a solar chimney, experimental data from a 12.3 m high prototype of a solar chimney was used. The tests were carried out over a 4-day period. The main points of the conclusion are

- the profiles of temperature and velocity are closely related to incident solar radiation on the device;
- the temperature defined for the dead state plays an important role in the exergy rates and exergetic efficiencies obtained. For a fixed temperature of the dead state (defined as the minimum ambient temperature of the whole test), it was found that the exergy rates and exergetic efficiencies were higher than those obtained with the instantaneous ambient temperature. This behaviour can be explained due to the lower reference environment;
- the higher exergy rates are found for the exergy flow rates due to heat transfer;
- lower exergy losses were found for the last day. Besides, the higher exergy losses were found close to 12:00. Therefore, it can be concluded that higher incident solar radiation levels lead to higher exergy losses. Higher solar radiation levels

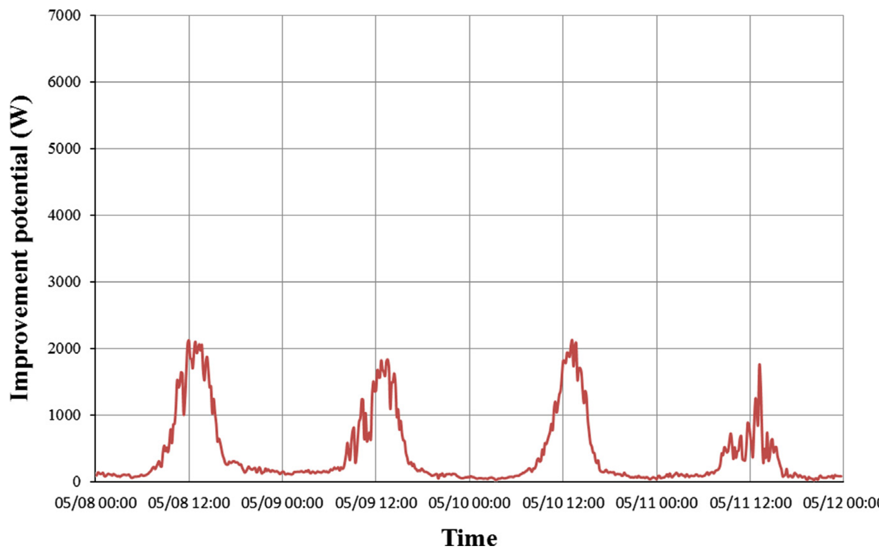


Fig. 14. Improvement potential as a function of time for the dead state selected with ambient temperature.

generate higher heat transfer rates to the airflow. Since this heat was not used, the exergy losses were higher, and the exergetic efficiencies were lower. In a solar chimney power plant or in a small prototype of a solar chimney used to dry agricultural products, higher solar radiation levels promote an increase in the power output and of the drying efficiency, respectively.

– The exergetic losses were very significant, mainly because the hot airflow generated was not used to drive a turbine, therefore there is a great potential of exergy to be harnessed.

Acknowledgements

The authors are thankful to CNPq, FAPEMIG, and PUC Minas.

References

[1] Xu G, Ming T, Pan Y, Meng F, Zhou C. Numerical analysis on the performance of solar chimney power plant system. Energy Conversion and Management 2011;52:876–83.
[2] Dai YJ, Huang HB, Wang NRZ. Case study of solar chimney power plants in North-western regions of China. Renewable Energy 2003;28:1295–304.
[3] Schlaich J. The solar chimney: electricity from the sun. Stuttgart: Axel Menges; 1995.
[4] Bernardes MAS, Von Backström TW. Evaluation of operational control strategies applicable to solar chimney power plants. Solar Energy 2010;84: 277–288.
[5] Haaf W, Friedrich K, Mayr G, Schlaich J. Solar chimneys, part I: principle and construction of the pilot plant in Manzanares. International Journal of Solar Energy 1983;2:3–20.
[6] Haaf W. Solar chimneys, part II: preliminary test results from the Manzanares pilot plant. IInternational Journal of Solar Energy 1984;2:141–61.
[7] Hamdan MO. Analysis of a solar chimney power plant in the Arabian Gulf region. Renewable Energy 2011;36:2593–8.
[8] Schlaich J, Schiel W. Solar chimneys. 3rd ed.Encyclopedia of physical science and technology, 3. London: Academic Press; 1–11.
[9] Schlaich J, Bergermann R, Schiel W, Weinrebe G. Sustainable electricity generation with solar updraft towers. Structural Engineering International 2004;3:225–9.
[10] Bernardes MA, dos S. Technische, ökonomische und ökologische Analyse von Aufwind-kraftwerken. Institut für Energiewirtschaft und Rationelle Energieanwendung. Germany: Universität Stuttgart; 2004.
[11] Fluri TP, Pretorius JP, Van Dyk C, Von Backström TW, Kröger DG, Van Zijl GPAG. Cost analysis of solar chimney power plants. Solar Energy 2009;83:246–56.
[12] Zhou X, Xiao B, Liu W, Guo X, Yang J, Fan J. A review of solar chimney power technology. Renewable and Sustainable Energy Reviews 2010;14: 2315–2338.
[13] Dincer I, Sahin AZ. A new model for thermodynamic analysis of a drying process. International Journal of Heat and Mass Transfer 2004;47:645–52.
[14] Kavak Akpinar E, Midilli A, Bicer Y. The first and second law analyses of thermodynamic of pumpkin drying process. Journal of Food Engineering 2006;72:320–31.
[15] Celma AR, Cuadros F. Energy and exergy analyses of OMW solar drying process. Renewable Energy 2009;34:660–6.
[16] Boulemtafes-Boukadoum A, Benzaoui A. Energy and exergy analysis of solar drying process of Mint. Energy Procedia 2011;6:583–91.
[17] Panwar NL, Kaushik SC, Kothari S. A review on energy and exergy analysis of solar dying systems. Renewable and Sustainable Energy Reviews 2012;16: 2812–2819.
[18] Saidur R, BoroumandJazi G, Mekhlif S, Jameel M. Exergy analysis of solar energy applications. Renewable and Sustainable Energy Reviews 2012;16:350–6.
[19] Aghbashlo M, Mobli H, Rafiee S, Madadlou A. A review on exergy analysis of drying processes and systems. Renewable and Sustainable Energy Reviews 2013;22:1–22.
[20] Petela R. Thermodynamic study of a simplified model of the solar chimney power plant. Solar Energy 2009;83:94–107.
[21] Bernardes MA, dos S, Valle RM, Cortez MFB. Numerical analysis of natural laminar convection in a radial solar heater. International Journal of Thermal Sciences 1999;38:42–50.
[22] Maia CB, Ferreira AG, Valle RM, Cortez MFB. Theoretical evaluation of the influence of geometric parameters and materials on the behavior of the airflow in a solar chimney. Computers and Fluids 2009;38:625–36.
[23] Chergui Larbi S, Bouhdjar A. Thermo-hydrodynamic aspect analysis of flows in solar chimney power plants – a case study. Renewable and Sustainable Energy Reviews 2010;14:1410–8.
[24] Vahl Davis G. Natural convection of air in a square cavity: a Benchmark numerical solution. International Journal for Numerical Methods in Fluids 1983;3:249–64.
[25] Pastohr H, Kornadt O, Gürlebeck K. Numerical and analytical calculations of the temperature and flow field in the upwind power plant. International Journal of Energy Research 2004;28:495–510.
[26] Ming T, Liu W, Pan Y, Xu G. Numerical analysis of flow and heat transfer characteristics in solar chimney power plants with energy storage layer. Energy Conversion and Management 2008;49:2872–9.
[27] Tingzhen M, Wei L, Guoling X, Yanbina X, Xuhua G, Yuan P. Numerical simulation of the solar chimney power plant systems coupled with turbine. Renewable Energy 2008;33:897–905.
[28] Koonsrisuk A, Chitsomboon T. Partial geometric similarity for solar chimney power plant modeling. Solar Energy 2009;83:1611–8.
[29] Koonsrisuk A, Chitsomboon T. A single dimensionless variable for solar chimney power plant modeling. Solar Energy 2009;83:2136–43.
[30] Sangi R, Amidpour M, Hosseinizadeh B. Modeling and numerical simulation of solar chimney power plants. Solar Energy 2011;85:829–38.
[31] Asnaghi A, Ladjevardi SM. Solar chimney power plant performance in Iran. Renewable and Sustainable Energy Reviews 2012;16:3383–90.
[32] Bernardes MA, dos S, Voβ A, Weinrebe G. Thermal and technical analyses of solar chimneys. Solar Energy 2003;75:511–24.
[33] Koonsrisuk A, Chitsomboon T. Accuracy of theoretical models in the prediction of solar chimney performance. Solar Energy 2009;83:1764–71.
[34] Pretorius JP, Kröger DG. Critical evaluation of solar chimney power plant performance. Solar Energy 2006;80:535–44.
[35] Fluri TP, Von Backström TW. Performance analysis of the power conversion unit of a solar chimney power plant. Solar Energy 2008;82:999–1008.
[36] Nizetic S, Klarin B. A simplified analytical approach for evaluation of the optimal ratio of pressure drop across the turbine in solar chimney power plants. Applied Energy 2010;87:587–91.

[37] Li J, Guo P, Wang Y. Effects of collector radius and chimney height on power output of a solar chimney power plant with turbines. Renewable Energy 2012;47:21–8.
[38] Hamdan MO. Analysis of solar chimney power plant utilizing chimney discrete model. Renewable Energy 2013;56:50–4.
[39] Koonsrisuk A, Chitsomboon T. Mathematical modeling of solar chimney power plants. Energy 2013;51:314–22.
[40] Maia CB, Ferreira AG, Valle RM, Cortez MFB. Analysis of the airflow in a prototype of a solar chimney dryer. Heat Transfer Engineering 2009;30:393–9.
[41] Ferreira AG, Maia CB, Cortez MFB, Valle RM. Technical feasibility assessment of a solar chimney for food drying. Solar Energy 2008;82:198–205.
[42] Kasaeian AB, Heidari E, Nasiri Vatan Sh. Experimental investigation of climatic effects on the efficiency of a solar chimney power plant. Renewable and Sustainable Energy Reviews 2011;15:5202–6.
[43] Sangi R. Performance evaluation of solar chimney power plants in Iran. Renewable and Sustainable Energy Reviews 2012;16:704–10.
[44] Gholamalizadeh E, Mansouri SH. A comprehensive approach to design and improve a solar chimney power plant: a special case – Kerman project. Applied Energy 2013;102:975–82.
[45] Zhou X, Yang J, Xiao B, Hou G. Simulation of a pilot solar chimney thermal power generating equipment. Renewable Energy 2007;32:1637–44.
[46] Zhou X, Yang J, Xiao B, Hou G. Experimental study of temperature field in a solar chimney power setup. Applied Thermal Engineering 2007;27:2044–50.
[47] Zhou X, Wang F, Fan J, Ochieng RM. Performance of solar chimney power plant in Qinghai–Tibet Plateau. Renewable and Sustainable Energy Reviews 2010;14:2249–55.
[48] Onyango FN, Ochieng RM. The potential of solar chimney for application in rural areas of developing countries. Fuel 2006;85:2561–6.
[49] Nizetic S, Ninic N, Klarin B. Analysis and feasibility of implementing solar chimney power plants in the Mediterranean region. Energy 2008;33:1680–90.
[50] Larbi S, Bouhdjar A, Chergui T. Performance analysis of a solar chimney power plant in the southwestern region of Algeria. Renewable and Sustainable Energy Reviews 2010;14:470–7.
[51] Ketlogetswe C, Fiszdon JK, Seabe OO. Solar chimney power generation project – the case for Botswana. Renewable and Sustainable Energy Reviews 2008;12:2005–12.
[52] Krisst RJK. Energy transfer system. Alternative Sources of Energy 1983;63:8–11.
[53] Kulunk H. A prototype solar convection chimney operated under Izmit conditions. In: Veziroglu TN., editors. In: Proceedings of the seventh MICAES; 1985. p. 162.
[54] Hepbasli A. A key review on exergetic analysis and assessment of renewable energy resources for a sustainable future. Renewable and Sustainable Energy Reviews 2008;12:593–661.
[55] Alpuche MG, Heard C, Best R, Rojas J. Exergy analysis of air cooling systems in buildings in hot humid climates. Applied Thermal Engineering 2005;25:507–17.
[56] Van Gool W. Energy policy: fairy tales and factualities. In: Soares ODD, Martins da Cruz A, Costa Pereira G, Soares IMRT, Reis AJPS, editors. Innovation and technology-strategies and policies. Dordrecht: Kluwer; 1997. p. 93–105.
[57] Duffie JA, Beckman WA. Solar engineering of thermal processes. 3rd ed. New York: John Wiley & Sons; 2006.
[58] Saidur R, BoroumandJazi G, Mekhlif S, Jameel M. Exergy analysis of solar energy applications. Renewable and Sustainable Energy Reviews 2012;16:350–6.
[59] Belessiotis V, Delyannis E. Solar drying. Solar Energy 2011;85:1665–91.